Electrochemical and Solid-State Letters, **11** (2) H36-H38 (2008)
1099-0062/2007/11(2)/H36/3/$23.00 © The Electrochemical Society

Possible Ohmic Mechanisms of Ag/Indium Tin Oxide p-Type Contacts for High-Brightness GaN-Based Light Emitting Diodes

June-O Song,[a] Hyun-Gi Hong,[b] Joon-Woo Jeon,[b] Jung-Inn Sohn,[c] Ja-Soon Jang,[d] and Tae-Yeon Seong[b,*,z]

[a]*National Institute for Materials Science, Tsukuba, Ibaraki 305-0044, Japan*
[b]*Department of Materials Science and Engineering, Korea University, Seoul 136-713, Korea*
[c]*Nanoscience Centre, University of Cambridge, Cambridge CB3 0FF, United Kingdom*
[d]*School of Electrical Engineering and Computer Science, Yeungnam University, Gyeongsangbuk-do 712-749, Korea*

We have investigated the Ag (1 nm)/indium tin oxide (ITO) (200 nm) contacts by scanning transmission electron microscopy (STEM), Auger electron spectroscopy (AES), and X-ray photoemission spectroscopy (XPS) to understand its ohmic mechanism. The Ag/ITO contacts exhibit ohmic behaviors, when annealed at 400–600°C. The effective Schottky barrier heights depend on the annealing temperatures. STEM and AES results reveal the formation of Ag nanodots (5–35 nm across) and Ga–Ag solid solution. Based on the STEM, AES, and XPS results, the ohmic contact formation is described in terms of the formation of the Ga–Ag solid solution and the inhomogeneous interfaces with nanodots.
© 2007 The Electrochemical Society. [DOI: 10.1149/1.2819536] All rights reserved.

Manuscript submitted October 2, 2007; revised manuscript received October 31, 2007. Available electronically December 5, 2007.

For solid-state lighting application, the fabrication of high-brightness GaN-based light emitting diodes (LEDs) is essential. In this regard, high external quantum efficiency must be achieved. To enhance the external quantum efficiency, transparent p-type ohmic electrodes having low contact resistance should be developed, because p-type ohmic contacts play a key role in enhancing LED performance.[1] For this purpose, different p-type ohmic schemes based on transparent conducting oxides (TCOs), such as indium tin oxide (ITO)[2-7] and ZnO,[8] have been widely investigated. However, TCO schemes were shown to produce good ohmic behavior, only when metal or additional TCO layers were inserted at the interfaces between TCOs and p-GaN. For example, Ni/ITO contacts resulted in ohmic characteristics with a specific contact resistance of $\sim 8 \times 10^{-4}\ \Omega\ cm^2$ and light transmittance of ~80% at wavelengths in the range of 450–550 nm, when annealed at 600°C in air.[3,4] It was also shown that use of electron-beam-evaporated NiO produces good ohmic behavior and LEDs fabricated with the NiO/ITO p-contacts give better performance compared to those with oxidized Ni/ITO contacts.[5] In addition, insertion of Au nanoparticles was shown to improve the electrical properties of ITO-based contacts to p-GaN.[6] Our group reported that the introduction of a 1 nm thick Ag interlayer is effective in forming highly transparent ITO ohmic contacts to p-GaN.[7] Ag/ITO contacts yielded a high transmittance of ~96% at a wavelength of 460 nm and a specific contact resistance as low as $1.2 \times 10^{-4}\ \Omega\ cm^2$ when annealed at 50°C for 1 min in air. LEDs fabricated with the Ag/ITO p-contacts showed much better output performance compared to LEDs with oxidized Ni/Au p-contacts. These results indicate that the interlayered TCO schemes could serve as promising p-type ohmic electrodes for high-brightness GaN-based LEDs. Despite the technological importance of these TCO-based p-contacts, however, their ohmic formation mechanisms have not been fully investigated thus far. In this work, we have investigated the electrical, structural, and chemical properties of Ag/ITO contacts to understand its possible ohmic mechanisms. It is shown that annealing the samples causes the formation of Ag nanodots and Ga–Ag solid solution, which could be responsible for the ohmic contact formation.

The 1.5 μm thick p-GaN layers (with a carrier concentration of $5 \times 10^{17}\ cm^{-3}$) that were grown by metallorganic chemical vapor deposition were ultrasonically degreased using trichloroethylene, acetone, methanol, and deionized (DI) water for 5 min in each step, followed by N_2 blowing. Prior to lithography, the GaN samples were treated with a buffered oxide etch (BOE) solution for 20 min and rinsed in DI water. Transfer length method (TLM) patterns were defined by the standard photolithographic technique for measuring specific contact resistances. The spacing between the TLM pads varied from 4 to 24 μm. Prior to metal deposition, all the samples were treated in a boiling BOE solution for 5 min.[9] Then, Ag (1 nm) and ITO (200 nm) layers were sequentially deposited by electron beam evaporation at a base pressure of 2×10^{-7} Torr and a working pressure of 8×10^{-5} Torr. Some of the samples were then rapid-thermal annealed at temperatures in the range 400–600°C for 1 min in air. Current-voltage (*I-V*) data were measured at room temperature using a parameter analyzer (HP 4155A), and Schottky barrier heights (SBHs) were calculated using *I-V* methods. Auger electron spectroscopy (AES) was performed using a PHI 670 Auger microscope with an electron beam of 10 keV and 0.0236 μA. X-ray photoemission spectroscopy [(XPS), VG Multilab ESCA 2000 model] was performed using a Mg Kα X-ray source in an ultrahigh vacuum system. The microstructures of samples were characterized by field-emission scanning transmission electron microscopy (STEM) equipped with energy dispersive spectroscopy (EDS) (Tecnai G2 F20) operated at 200 kV.

I-V characteristics of Ag (1 nm)/ITO (200 nm) contacts were measured as a function of the annealing temperature, as shown in Fig. 1.[7] The as-deposited sample shows nonlinear *I-V* behavior. However, annealing significantly improves their *I-V* characteristics. The specific contact resistances of the samples were determined from a plot of the measured resistances vs the spacing between the TLM pads. The least-squares method was used to fit a straight line to the experimental data. Measurements showed that the contact resistivities are of the order of $10^{-4}\ \Omega\ cm^2$. The sample annealed at 500°C exhibits the lowest resistivity of $1.2 \times 10^{-4}\ \Omega\ cm^2$. Multiple quantum well InGaN/GaN blue LEDs fabricated using the 500°C-annealed Ag/ITO p-contacts gave forward-bias voltages similar to that of LEDs with oxidized Ni/Au contacts. However, because of their much higher transmittance (96% at 460 nm), LEDs with the Ag/ITO contacts produced much higher light output compared to LEDs with the oxidized Ni/Au contacts.[7]

In order to understand possible ohmic mechanisms of the Ag/ITO contacts, their effective SBHs are measured by means of the *I-V* method.[10,11] Figure 2 shows a plot of $I/[1 - \exp(-qV/kT)]$ vs V for the samples before and after annealing at 500°C. The SBH of the as-deposited sample is measured to be 0.477 eV. Annealing causes reduction of the SBHs, although the reduction depends on the temperature. The SBHs are 0.447, 0.437, and 0.443 eV for the samples

* Electrochemical Society Active Member.
z E-mail: tyseong@korea.ac.kr

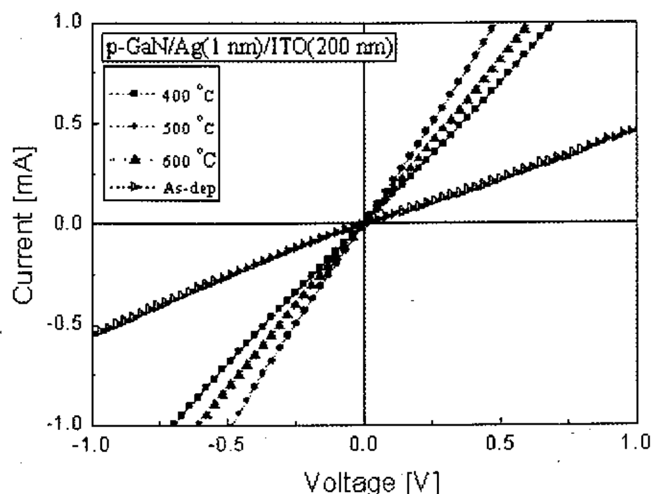

Figure 1. (Color online) *I-V* characteristics of Ag (1 nm)/ITO (200 nm) contacts measured as a function of the annealing temperature.

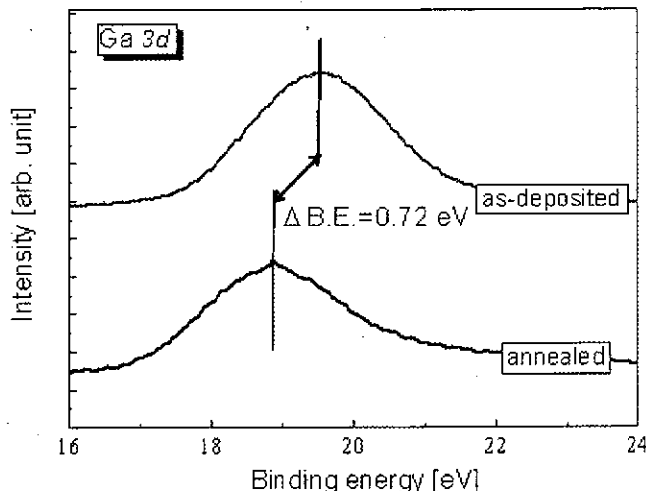

Figure 3. (Color online) The Ga 3d core level for the contact/GaN interface regions before and after annealing.

annealed at 400, 500, and 600°C, respectively. It is worth noting that the variation of the SBHs is consistent with the temperature dependence of the *I-V* characteristics (Fig. 1).

To characterize the chemical bonding state of Ga, XPS examination was made of the Ag/ITO contact samples on p-GaN before and after annealing at 500°C. Before starting analysis, the ITO layer was sputtered using Ar^+ ions to expose the interface region between the contact layer and GaN. Figure 3 shows the Ga 3d core level for the contact/GaN interface regions before and after annealing. It is evident that the Ga 3d core level for the annealed sample shifts toward the lower energy side by 0.72 eV compared to the as-deposited sample. This indicates that annealing causes a shift of the surface Fermi level toward the valence bandedge and, hence, the reduction of band bending in p-type material.[9,12-14]

The interface structures of the sample annealed at 500°C were characterized by STEM Z-contrast and EDS examinations. STEM results revealed the formation of Ag nanodots at the ITO/GaN interface. The Ag nanodots were measured to be 5–35 nm in size, as shown in a STEM Z-contrast image (Fig. 4), which was also confirmed by EDS and AES results.

Figure 5 shows plan-view AES mapping results obtained from the sample annealed at 500°C. It is clearly shown that Ag nanodots are randomly distributed on the GaN. (However, their shape is not bloblike. This might be because the Ag nanodots were sputtered away during AES examination.) Interestingly, there are also a number of Ga nanodots; their locations are exactly overlapped with the Ag nanodots. This can be attributed to the fact that Ga atoms outdiffuse into the Ag nanodots to form Ag–Ga solid solution, as demonstrated by our previous work.[15] This is indicative of the generation of Ga vacancies near the GaN surface region.

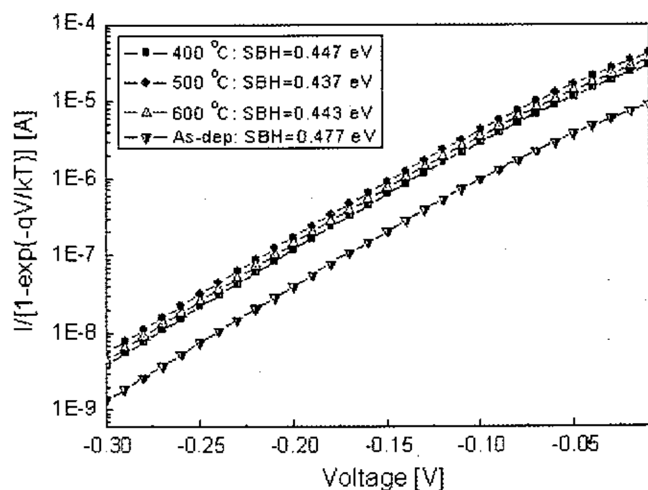

Figure 2. (Color online) Plot of $I/[1 - \exp(-qV/kT)]$ vs V for the samples before and after annealing at 500°C.

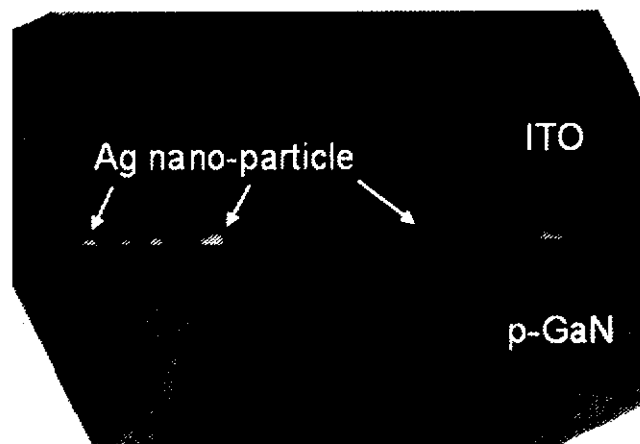

Figure 4. STEM Z-contrast and EDS results of the sample annealed at 500°C. The STEM results show the formation of Ag nanodots (5–35 nm in size) at the ITO/GaN interface.

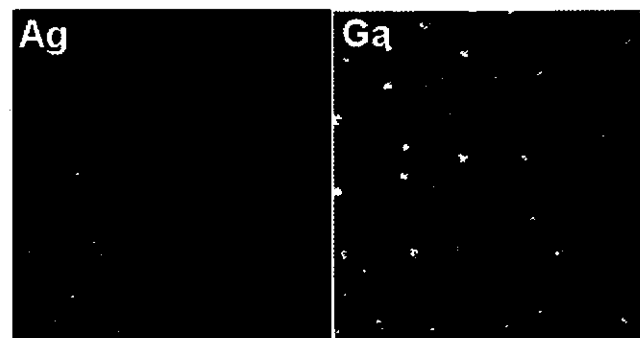

Figure 5. (Color online) Plan-view AES mapping results obtained from the sample annealed at 500°C.

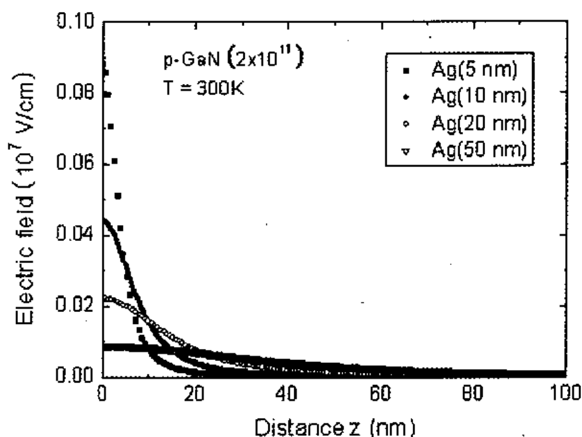

Figure 6. (Color online) The calculated electric field distribution vs distance (z) from the MS interface to the inside of GaN for the samples as a function of the size of Ag nanodots.

It was shown that the Ag (1 nm) and ITO (200 nm) contacts produce good ohmic behaviors, when annealed, in particular, at 500°C. This is contrary to the results obtained from ITO single p-contacts, which produce rectifying characteristics upon annealing.[16] In fact, the annealed ITO scheme was reported to form ohmic contacts to n-type GaN, but not p-type GaN.[16] The annealing-induced improvement of the electrical properties of the Ag/ITO contacts could be explained as follows. First, the improvement could be associated with the formation of Ag–Ga solid solution,[15,17,18] as noted from the AES result. The formation of the Ag–Ga solid solution produces deep acceptorlike Ga vacancies near the GaN surface region under the contacts, resulting in an increase of carrier concentration at the surface region and so the reduction of band bending in p-type material.[12-14] Second, the improvement may be related to the formation of the contact scheme/GaN interface with inhomogeneous Schottky barriers due to the breaking up of Ag interlayers, as shown by the STEM (Fig. 4) and AES result (Fig. 5). The electronic transport theory at the metal/semiconductor (MS) interface with inhomogeneous SBHs shows that the electric field for circular patch geometry (e.g., nanodot) at the MS interface is given by[19]

$$E(z) = V_{bi}\left(\frac{2}{w} - \frac{2z}{w^2}\right) - \Delta\phi_{\text{ITO-Ag}}\left[\frac{1}{(z^2 + R_o^2)^{1/2}} - \frac{z^2}{(z^2 + R_o^2)^{3/2}}\right] \quad [1]$$

where V_{bi} is the band bending, z is the distance from the surface of the semiconductor, w is the depletion width, R_o is the radius of the circular patch (i.e., Ag nanodot), and $\Delta\phi_{\text{ITO-Ag}}$ is the SBH difference resulting from the different work functions of ITO and Ag. The first term on the right-hand side of Eq. 1 implies the electric field due to a uniform SBH, and the second term indicates the variation of the electric field due to the presence of nanodots.

Figure 6 shows the calculated electric field distribution vs distance (z) from the MS interface to the inside of GaN for the samples as a function of the size of Ag nanodots. The values used for this calculation are obtained from Ref. 20-23. It is worth noting that the electric field at the MS interface increases exponentially with decreasing size of the nanodots. Equation 1 and Fig. 6 demonstrate that the difference in the SBHs of ITO and Ag, and the presence of the interfacial Ag nanodots can increase the electric field at the MS interface. It was shown that the increase of the electric field brings about a lowering of a barrier height.[12,24] Equation 1 also shows that the presence of the Ag nanodots could cause the reduction of the SBHs.

To summarize, we investigated the ohmic formation mechanism of the Ag/ITO contacts to p-GaN. STEM results revealed the formation of interfacial Ag nanodots (5–35 nm across). Measurements using the I-V methods showed that the annealed samples give lower SBHs than the as-deposited sample. The STEM, AES, and XPS results showed that the formation of Ga–Ag solid solution (Ag nanodots) and the inhomogeneous interfaces with nanodots having a different work function could be responsible for the ohmic formation and may serve as a design tool for the formation of p-type ohmic electrodes for GaN-based LEDs.

Acknowledgment

This work was supported by the basic research program of the Korea Science and Engineering Foundation (grant no. R01-2006-000-10904-0).

Korea University assisted in meeting the publication costs of this article.

References

1. J.-S. Jang, I.-S. Chang, H.-K. Kim, T.-Y. Seong, S. Lee, and S.-J. Park, *Appl. Phys. Lett.*, **74**, 70 (1999).
2. T. Margalith, O. Buchinsky, D. A. Cohen, A. C. Abare, M. Hansen, S. P. DenBaars, and L. A. Coldren, *Appl. Phys. Lett.*, **74**, 3930 (1999).
3. R.-H. Horng, D.-S. Wuu, Y.-C. Lien, and W.-H. Lan, *Appl. Phys. Lett.*, **79**, 2925 (2001).
4. Y. C. Lin, S. J. Chang, Y. K. Su, T. Y. Tsai, C. S. Chang, S. C. Shei, H. J. Hsu, C. H. Liu, U. H. Liaw, S. C. Chen, et al., *Photon. Technol. Lett.*, **14**, 1668 (2002).
5. S.-M. Pan, R.-C. Tu, Y.-M. Fan, R.-C. Yeh, and J.-T. Hsu, *Photon. Technol. Lett.*, **15**, 646 (2003).
6. Lung-Chien Chen and Seng-Fong Lu, *Phys. Status Solidi A*, **203**, 2451 (2006).
7. J.-O. Song, D.-S. Leem, J. Kwak, Y. Park, S. W. Chae, and T.-Y. Seong, *Photon. Technol. Lett.*, **17**, 291 (2005).
8. J.-O. Song, K.-K. Kim, S.-J. Park, and T.-Y. Seong, *Appl. Phys. Lett.*, **83**, 479 (2003).
9. J.-S. Jang, S.-J. Park, and T.-Y. Seong, *J. Vac. Sci. Technol. B*, **17**, 2667 (1999).
10. T. Mori, T. Kozawa, T. Ohwaki, Y. Taga, S. Nagai, S. Yamasaki, S. Asami, N. Shibata, and M. Koike, *Appl. Phys. Lett.*, **69**, 3537 (1996).
11. E. H. Rhoderick and R. H. Williams, *Metal-Semiconductor Contacts*, Clarendon, Oxford (1988).
12. J.-O. Song, D.-S. Leem, and T.-Y. Seong, *Appl. Phys. Lett.*, **83**, 3513 (2003).
13. J. S. Jang and T.-Y. Seong, *J. Appl. Phys.*, **88**, 3064 (2000).
14. V. M. Bermudez, D. D. Koleske, and A. E. Wickenden, *Appl. Surf. Sci.*, **126**, 69 (1998).
15. J.-O. Song, J. S. Kwak, Y. Park, and T.-Y. Seong, *Appl. Phys. Lett.*, **86**, 062104 (2005).
16. J. K. Sheu, Y. K. Su, G. C. Chi, M. J. Jou, and C. M. Chung, *Solid-State Electron.*, **43**, 2081 (1999).
17. D.-S. Leem, J.-O. Song, H.-G. Hong, J. S. Kwak, Y. Park, and T.-Y. Seong, *Electrochem. Solid-State Lett.*, **7**, G219 (2004).
18. J.-O. Song, D.-S. Leem, J. S. Kwak, O. H. Nam, Y. Park, and T.-Y. Seong, *Photon. Technol. Lett.*, **16**, 1450 (2004).
19. R. T. Tung, *Mater. Sci. Eng., R.*, **35**, 1 (2001).
20. A. L. Dawn, A. K. Jain, C. Jagadish, and H. L. Hartnagel, *Semiconducting Transparent Thin Films* IOP, London (1995).
21. S. Nakamura, S. Pearton, and G. Fasol, *The Blue Laser Diode*, Springer, Heidelberg (2000).
22. H. B. Michaelson, *J. Appl. Phys.*, **48**, 4729 (1977).
23. T. J. Marks, J. G. C. Veinot, J. Cui, H. Yan, A. Wang, N. L. Edleman, J. Ni, Q. Huang, P. Lee, and N. R. Armstrong, *Synth. Met.*, **127**, 29 (2002).
24. J.-I. Sohn, J.-O. Song, D.-S. Leem, S. Lee, and T.-Y. Seong, *Electrochem. Solid-State Lett.*, **7**, G179 (2004).